12-20-2002

Chaotic Free-Space Laser Communication over Turbulent Channel

N. F. Rulkov
University of California - San Diego

Mikhail Vorontsov
University of Dayton, mvorontsov1@udayton.edu

L. Illing
University of California - San Diego

Chaotic Free-Space Laser Communication over a Turbulent Channel

N. F. Rulkov,[1] M. A. Vorontsov,[2] and L. Illing[1]
[1]Institute for Nonlinear Science, University of California, San Diego, La Jolla, California 92093
[2]Army Research Laboratory, Adelphi, Maryland 20783
(Received 2 May 2002; published 20 December 2002)

The dynamics of errors caused by atmospheric turbulence in a self-synchronizing chaos-based communication system that stably transmits information over a ~5 km free-space laser link is studied experimentally. Binary information is transmitted using a chaotic sequence of short-term pulses as a carrier. The information signal slightly shifts the chaotic time position of each pulse depending on the information bit. We report the results of an experimental analysis of the atmospheric turbulence in the channel and the impact of turbulence on the bit-error-rate performance of this chaos-based communication system.

DOI: 10.1103/PhysRevLett.89.277905 PACS numbers: 05.45.Vx, 42.68.Bz, 42.60.By

Studies of chaos in nonlinear electrical circuits [1] and lasers [2] have shown that chaotic signals generated in these systems can potentially be used as carriers for information transmission. Thanks to the deterministic origin of chaos, two coupled chaotic systems can self-synchronize reproducing at the receiver end the chaotic waveforms generated in the transmitter [3]. This regime of self-synchronization is a key element in the recovery of information encoded in the received chaotic signal [4]. Because of the variety and complexity of the nonlinear dynamical issues involved, such chaos-based communication systems are of broad interest both for theoreticians and experimentalists [5].

All practical communication channels introduce signal distortions that alter the chaotic waveform shape; as a result, the received chaotic oscillations do not precisely represent the transmitter oscillations. Channel noise, filtering, attenuation variability, and other distortions in the channel corrupt the chaotic carrier and information signal. The presence of these channel distortions significantly hampers the onset of identical synchronization of the chaotic systems [6]. When signal distortions in the channel exceed a certain level, self-synchronizing fails resulting in failure of the communication link.

The enhanced sensitivity to chaotic signal waveform shape distortions and the resulting problems with chaos synchronization remain the major problems in the studies of chaos-based communication systems. In order to overcome the problems of channel distortions, a number of special chaotic communication methods have been proposed [7]. At least in theory and numerical simulations, it appears that the regime of identical synchronization in these specially designed systems is significantly less sensitive to channel noise and waveform distortions caused by limited bandwidth of the channel [8]. However, to the best of our knowledge, self-synchronizing chaos communication over a real-life highly nonstationary channel has not been demonstrated so far.

In this Letter we report the experimental study of a chaotic self-synchronizing free-space laser communication in the presence of severe communication signal distortions caused by atmospheric turbulence. Chaotic pulse signals were used as the optical communication carrier. Results demonstrate reliable self-synchronization of two coupled chaotic systems for most of the time and reveal the dynamical properties of errors bursts. Synchronization failed only when deep signal fading occurred so that the received power decreased to the photoreceiver noise level.

A schematic representation of the chaotic free-space laser communication system used is shown in Fig. 1. The intensity-modulated 10 mW semiconductor laser beam ($\lambda = 690$ nm) coupled to a single-mode fiber. Using a lens relay system (lenses L_1 and L_2) and the transmitter telescope (Celestron) the beam from the fiber was expanded to a 4 in. diameter. The laser beam propagation

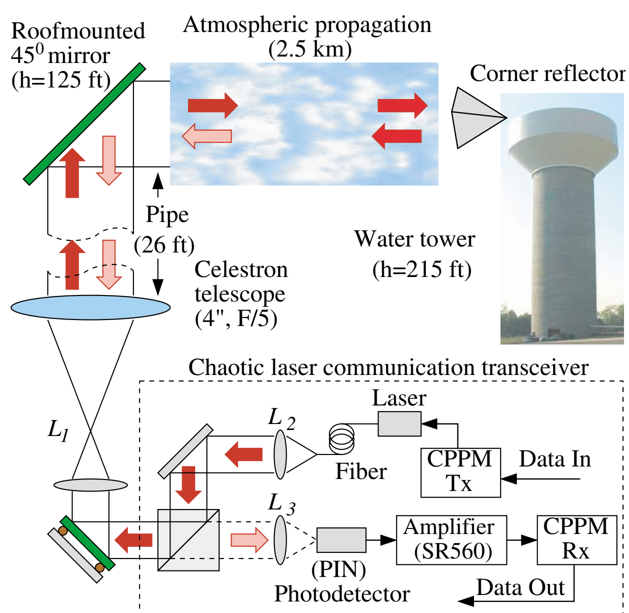

FIG. 1 (color online). Schematic for the free-space laser communication system based on the chaotic pulse position modulation transceiver. See text.

path included a 26 ft long vertical air-locked pipe connecting the optical table with a 45° mirror placed inside a shed on the roof of the building, with subsequent propagation over an atmospheric path of length $L \simeq 2.5$ km. At the end of the propagation path was a 4 in. corner cube reflector placed on top of a water tower. After reflection the laser beam propagated from the water tower back to a communication receiver telescope in the roof-mounted shed. The receiver system used the same Celestron telescope and lens relay system (lenses L_1 and L_3) as did the transmitter system. The total double-pass atmospheric laser beam propagation distance was approximately $2L \simeq 5$ km long.

Double-pass wave propagation in a medium with random refractive index fluctuations displays interesting statistical properties known as backscatter enhancement. Backscatter enhancement results from correlations in the wave front phase aberrations between the outgoing and returned waves which have propagated through the same refractive index inhomogeneities [9,10]. The variance of the received wave phase and intensity fluctuation enhancement can exceed the corresponding value for a unidirectional wave that propagates the distance $z = 2L$ in an optically inhomogeneous medium. Under conditions of strong intensity fluctuations the backscatter enhancement factor can exceed a factor of 2 [11].

The received laser beam power was registered by the positive-intrinsic-negative (PIN) photodetector (PDA55) placed in the lens L_3 focal plane (Fig. 1). To evaluate the level of intensity scintillations in the channel we examined the received signal from a continuously running laser with a steady output intensity. An example of the received signal fluctuations, measured by the PIN photodetector, amplified by the low-noise preamplifier (SR560 with a gain of 20), and then acquired with sampling rate 1000 samples/sec, is presented in Fig. 2(a).

The received signal standard deviation normalized by the mean value is as high as 0.8–0.9, which is indicative of a *strong scintillation regime* [10]. The corresponding ensemble-averaged received signal power spectrum S_{P_R} is shown in Fig. 2(b). In atmospheric optics, laser beam intensity scintillations are traditionally described in terms of the logarithm of the normalized intensity I (for a point receiver) or received power P (for a finite receiver telescope): $\xi_I = \ln(I) - \ln\langle I\rangle$ or $\xi_P = \ln(P) - \ln\langle P\rangle$, where $\langle I\rangle$ and $\langle P\rangle$ are ensemble (time) averaged values [10,12]. A histogram that represents the distribution of the values of random variable ξ_P normalized by the total number of samples N is shown in Fig. 3. Representing an approximation of the received power probability distribution, the histogram in Fig. 3 closely matches the log-normal distribution expected from theory [10].

In the experiment with a chaotic transceiver the laser generated a chaotic sequence of short-term ($\sim 1.0\ \mu$s) on-off pulses of intensity $U(t) = \sum_{j=0}^{\infty} w(t - t_j)$. Here $w(t - t_j)$ represents the waveform of an individual

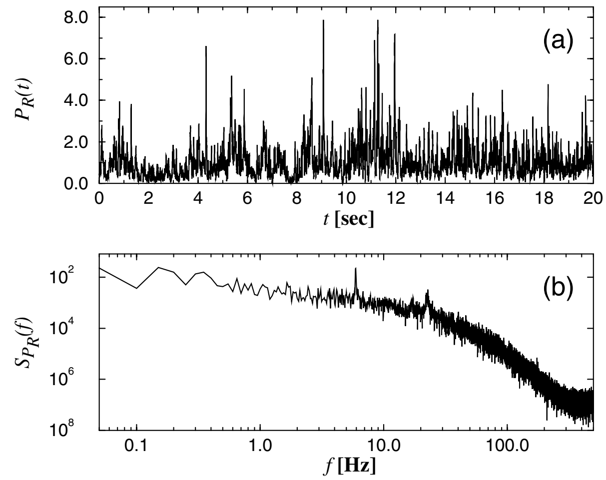

FIG. 2. Fluctuations of the received power $P(t)$ in the experiment with a nonmodulated laser generating constant output intensity (10 mW). Normalized received power $P_R(t) = P(t)/\langle P(t)\rangle$ measured at the photodetector output (a), and corresponding averaged power spectrum of $P_R(t)$ (b) illustrate the presence of strong laser beam intensity scintillations.

short-term rectangular pulse generated at the moment of time $t_j = t_0 + \sum_{n=0}^{j} T_n$, where T_n is the chaotic time interval between the nth and the $(n-1)$th pulse. The laser pulses were triggered by a transistor-transistor logic (TTL) pulse signal from the chaotic transceiver controller CPPM Tx (see Fig. 1). The chaotic sequence of the time intervals $\{T_n\}$ corresponds to iterations of a chaotic process with the binary information signal added to the chaotic signal. This method of chaos communication is referred to as chaotic pulse position modulation (CPPM) [13]. Since both chaos and information are in the timing of the pulses, the particular intensity waveform of the generated light pulses is of little consequence.

In the communication system discussed here the chaos is produced by iterations of a one-dimensional tent map

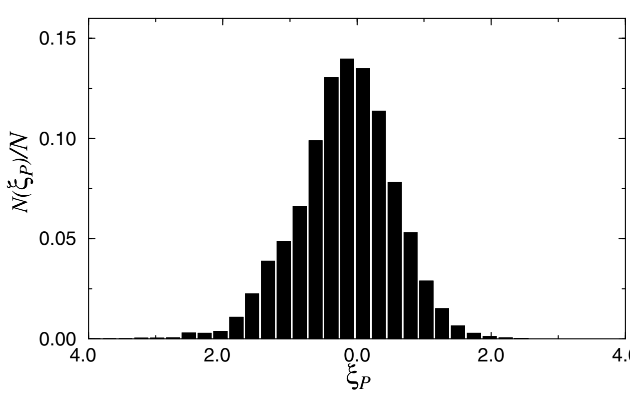

FIG. 3. Histogram of the probability distribution for the random variable $\xi_P = \ln(P/\langle P\rangle)$ measured by the PIN photodetector. This histogram, $N(\xi_P)/N$, is computed using $N = 10^5$ consecutive samples of the data $P(t)$, a 20 sec fragment of which is shown in Fig. 2.

(see [13] for details of the hardware design). Time intervals in the generated pulse sequence can be represented in the form of the following iterative map:

$$T_n = F(T_{n-1}) + d + mS_n, \tag{1}$$

where $F(\cdot)$ is a nonlinear function of the tent map and S_n is the binary information signal equal to either zero or 1. The parameter m characterizes the modulation amplitude whereas the parameter d is a constant time delay needed for the practical implementation. The nonlinear function $F(\cdot)$ and parameters d and m were tuned to achieve a robust regime of the map's chaotic behavior. The interpulse intervals $\{T_n\}$ fluctuated chaotically ranging from 10 to 25 μsec and supported a ~60 kbit per sec bit rate.

The distorted chaotic pulses $U'(t)$ received at the PIN photodetector are applied to CPPM Rx (see Fig. 1). Because of the channel distortions and filtering in the PIN detector the received pulses become a bell-shaped waveform. Each received pulse triggered a timer circuit in CPPM Rx, when its amplitude exceeded a certain threshold level, and the receiver acquired two consecutive time intervals T_{n-1} and T_n. The information signal was recovered from the chaotic iterations $\{T_n\}$ using formula [14]:

$$mS_n = [T_n - F(T_{n-1}) - d]. \tag{2}$$

Since the chaotic decoder map in the receiver is matched to the encoder map in the corresponding transmitter, the time of the next arriving pulse can be predicted [see Eq. (1)]. To improve system performance by reducing the probability of the channel noise falsely triggering the decoder, the input of the synchronized receiver was blocked until the moment of time when the next pulse was expected [13].

Because of the effects of atmospheric turbulence the received pulses were highly distorted. To illustrate, Fig. 4(a) shows the received pulse amplitude A_p as a function of time. Despite the severe pulse amplitude fluctuations clearly visible in Fig. 4(a), the pulse propagation time τ_m, which is measured between the leading front of the TTL pulse applied to the laser and the maximal point of the received pulse, varied only within a 0.2 μsec time interval; see Fig. 4(b). Small fluctuations of the propagation time in the turbulent channel are a potential for very good performance of the CPPM communication method. However, CPPM Rx is triggered when the leading front of the received bell-shaped pulse waveform crosses the threshold level. This level (~ 200 mV) was selected to minimize instances of receiver controller triggering caused by noise, or by pulses originating from local pulse reflections off nearby optical surfaces. Therefore, the actual delay time τ_t, measured between the leading front of TTL pulses generated by CPPM Tx and the moments of CPPM Rx triggering, depends on the amplitude of the received pulses and fluctuates; see Fig. 4(c). Gaps in the plots of τ_m and τ_t data occur due to the pulse amplitude fading when the pulse amplitude falls to the photoreceiver noise level and below the threshold level, respectively. Although τ_t changes with the amplitude variation these changes remain less than the modulation amplitude $m \sim 1.5$ μsec; see Eq. (1). Slow and small variation in the pulse propagation time is the key for CPPM controller self-synchronization, and hence for stability of the entire communication link.

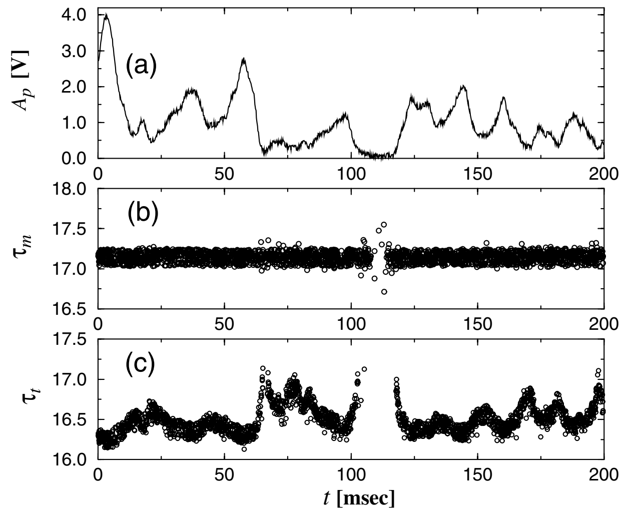

FIG. 4. Fluctuations of the CPPM pulses of light intensity after traveling through atmospheric turbulence. Pulse amplitude A_p measured in volts at the output of amplifier (a). Propagation times τ_m (b) and τ_t (c) in μsec. The pulse propagation times are computed from data acquired simultaneously at the output of CPPM Tx and output of amplifier (SR560) at a sampling rate of 5×106 samples per sec.

The dynamics of errors caused by the atmospheric turbulence was studied in the regime of real time transmission of binary pseudorandom code data. An example of a map of the lost data in such a transmission is presented in Fig. 5. The total bit-error rate (BER) measured in the experiment is 1.92×10^{-2}. From the detailed analysis of the error structure we conclude that main contributions to the BER are as follows. First, the loss of bits carried by the pulses which did not trigger the CPPM receiver due to the fading in the channel contributes $\sim 1.78 \times 10^{-2}$ to the BER (~ 92.7%). The fading moments occur randomly during the communication and cause the dropouts of blocks of data up to 1000 consecutive bits. The second group of errors occurs in the relatively short time intervals right before and after the failure of communication by fading. In these time intervals the amplitude of the received pulses is still close to the threshold and, as a consequence, even small noise in the channel can result in significant fluctuation of the interpulse intervals [see Fig. 4(c)]. This effect contributes $\sim 1.4 \times 10^{-3}$ to the BER (~ 7.3%). These two fading related error contributions would cause data loss not only in this *chaos*-based communication system but would equally affect a similar type of *periodic* pulse

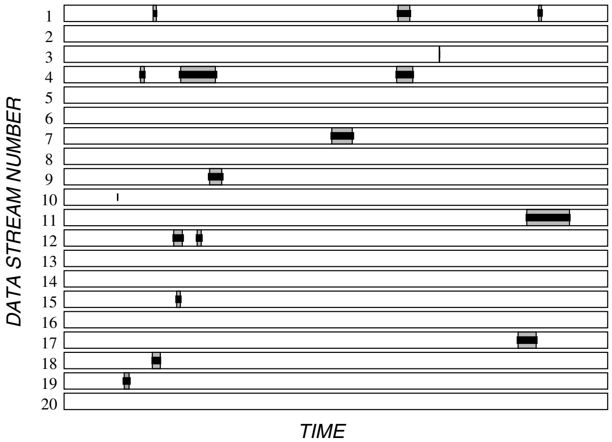

FIG. 5. Typical structure of errors shown in 20 consecutive measured data streams each of length ~170 m sec transmitted at ~2 min intervals. Each strip presents 10 000 bits which are transmitted with the CPPM method. White intervals of the strips mark blocks of data received without errors. Narrow black ribbons in the middle of the strips mark the blocks of data received with errors. The gray background shows the blocks of the dropped-out data caused by the loss of CPPM pulses due to fading instances.

position system. The rest of the errors which are not related to the complete failure of the channel by the fading instances and can therefore be associated with the susceptibility of the *chaos* communication to the channel distortions contributed to the BER only $\sim 5.5 \times 10^{-5}$.

This structure of errors indicates that the CPPM communication method supports robust communications over the turbulent channel except for the time intervals when the channel fails due to fading. Thanks to the self-synchronizing feature of this chaos communication method after the total fading phase is over the CPPM receiver resynchronizes fast. In fact it needs to receive only two correct pulses to establish the regime of chaos synchronization (see [13] for details).

The authors are grateful to L. S. Tsimring, H. D. I. Abarbanel, L. Larson, and A. R. Volkovskii for helpful discussions. This work was supported in part by the U.S. Department of Energy (Grant No. DE-FG03-95ER14516) and the U.S. Army Research Office (MURI Grant No. DAAG55-98-1-0269). The authors also thank J. Gowens and J. Carrano for support in the development of the Atmospheric Laser Optics Testbed (A_LOT) at Adelphi, Maryland used in the experiments.

[1] K. M. Cuomo and A.V. Oppenheim, Phys. Rev. Lett. **71**, 65 (1993); L. Kocarev *et al.*, Int. J. Bifurcation Chaos Appl. Sci. Eng. **2**, 709 (1992); T. L. Carroll and L. M. Pecora, IEEE Trans. Circuits Syst. **40**, 646 (1993); T. L. Carroll, Phys. Rev. E **53**, 3117 (1996); C.W. Wu and L. O. Chua, Int. J. Bifurcation Chaos Appl. Sci. Eng. **3**, 1619 (1993).

[2] P. Colet and R. Roy, Opt. Lett. **19**, 2056 (1994); P. Celka, IEEE Trans. Circuits Syst. **42**, 455 (1995); **43**, 869 (1996); C. R. Mirasso, P. Colet, and P. Garcia-Fernández, Photonics Technol. Lett. **8**, 299 (1996); G. D. VanWiggeren and R. Roy, Science **279**, 1198 (1998); Phys. Rev. Lett. **81**, 3547 (1998); H. D. I. Abarbanel and M. B. Kennel, Phys. Rev. Lett. **80**, 3153 (1998).

[3] H. Fujisaka and T. Yamada, Prog. Theor. Phys. **69**, 32 (1984); L. M. Pecora and T. L. Carroll, Phys. Rev. Lett. **64**, 821 (1990).

[4] D. R. Frey, IEEE Trans. Circuits Syst. **40**, 660 (1993); A. R. Volkovskii and N. F. Rulkov, Tech. Phys. Lett. **19**, 71 (1993); U. Feldmann, M. Hasler, and W. Schwarz, Int. J. Circuit Theory Appl. **24**, 551 (1996); L. Kocarev and U. Parlitz, Phys. Rev. Lett. **74**, 5028 (1995).

[5] See, for example, special focus issues: IEEE Trans. Circuits Syst. **48**, No. 12 (2001); Chaos **6**, No. 3 (1996); Chaos **7**, No. 4 (1997); Int. J. Bifurcation Chaos Appl. Sci. Eng. **10**, Nos. 11&12 (1993); Int. J. Circuit Theory Appl. **27**, No. 6 (1999).

[6] G. Kolumban, M. P. Kennedy, and L. O. Chua, IEEE Trans. Circuits Syst. **45**, 1129 (1998); C. Williams, IEEE Trans. Circuits Syst. **48**, 1394 (2001).

[7] T. L. Carroll, Phys. Rev. E **53**, 3117 (1996); T. L. Carroll and G. A. Johnson, Phys. Rev. E **57**, 1555 (1998); E. Rosa, S. Hayes, and C. Grebogi, Phys. Rev. Lett. **78**, 1247 (1997); H. Torikai, T. Saito, and W. Schwartz, IEEE Trans. Circuits Syst. **46**, 1072 (1999).

[8] T. L. Carroll, IEEE Trans. Circuits Syst. **42**, 105 (1995); **48**, 1519 (2001); N. F. Rulkov and L. Tsimring, Int. J. Circuit Theory Appl. **27**, 555 (1999).

[9] Yu. A. Kravtsov, Appl. Opt. **32**, 2681 (1993).

[10] L. C. Andrews, R. L. Phillips, and C. Y. Hopen, in *Laser Beam Scintillation with Applications*, SPIE Proceedings (SPIE–International Society for Optical Engineering, Bellingham, WA, 2001).

[11] Yu. A. Kravtsov and A. I. Saichev, Sov. Phys. Usp. **25**, 494 (1982).

[12] S. M. Rytov, Yu. A. Kravtsov, and V. I. Tatarskii, *Principles of Statistical Radiophysics, Wave Propagation through Random Media* (Springer-Verlag, Berlin, 1989).

[13] M. M. Sushchik, *et al.*, IEEE Commun. Lett. **4**, 128 (2000); N. F. Rulkov, *et al.*, IEEE Trans. Circuits Syst. **48**, 1436 (2001).

[14] In the CPPM Tx and CPPM Rx devices the consecutive values of T_n and T_{n-1} are generated and stored in the form of voltage signals. Equations (1) and (2) are implemented using an analog electrical circuit of the nonlinear function $F(\cdot)$ and a subtracting circuit; see Ref. [13] for details.